Improvement in surface properties with TiN thin film coating on plasma nitride austenitic 316 stainless steel

Pankaj Kumar Singh[δ1,#2], Arbind Kumar[#2], Sanjay Kumar Sinha[α3], Aman Aggarwal[Ψ4], Gajendra Prasad Singh*[5]

[δ]Department of Mechanical and Automation Engineering,
Amity School of Engineering and Technology, Bijwasan, New Delhi, India
[#]Department of Mechanical Engineering, Birla Institute of Technology, Mesra, Ranchi, Jharkhand, India
[1]pankajsinghps@gmail.com
[α]Department of Physics, Birla Institute of Technology, Mesra, Ranchi, Jharkhand, India
[Ψ]Department of Mechanical Engineering, Ganga Institute of Technology, Harayana, India
*Centre for Nanotechnology, Central University of Jharkhand, Brambe, Ranchi, Jharkhand, India
[5]gpsinghcuj@gmail.com

Abstract - The surface of the austenitic 316 stainless steel was modified by using two processes, i.e, dc glow discharge plasma and RF magnetron sputtering. The plasma nitriding was carried out at 500°C under 3 mbar pressure for 5 h in presence of $4N_2$:$1H_2$ gas mixture. A thin layer of TiN was coated on plasma nitrided samples by using RF magnetron sputtering.The phase formation, nitride layer, surface nanohardness and corrosion current density were evaluated by X-ray diffractogram, optical microscope and SEM, nanoindenter and electrochemical analyser. The untreated sample showed only γFe diffraction pattern while after nitriding CrN phase with γFe and after coating only TiN phase diffraction pattern is observed. The nitride layerof about 8-10 µm is observed in nitrided sample and TiN layer of about 200 nm is measured in TiN coated plasma nitride sample.The untreated 316 steel shows the surface nanohardness about 1. 59 to 1.88 GPa. The nitriding improved the surface hardness about five times (8.45GPa) and TiN coating further enhanced the surface hardness about seven times (13.16GPa) than untreated sample. The corrosion potential (E_{Corr}) of the plasma nitrided and TiN coated plasma nitrided 316 samples showing positive shift with reference to the untreated sample. The corrosion potential(E_{Corr}) value of untreated, plasma nitride and TiN coated plasma nitrided 316 samples are -0.593 V, -0.443 V and 0.074 V, respectively. The corrosion current density (I_{Corr}) is considerably enhanced after nitriding and TiN coating, i.e., 4.46 µAcm^{-2} and 2.24 µAcm^{-2} respectively than 15.13 µAcm^{-2} for untreated sample. The passivation current densities of samples measured at 0.6 V vs SHEare about 69.18 µAcm^{-2}, 18.62 µAcm^{-2} and 3.16µAcm^{-2}, respectively.

Keyword – TiN coating, Nitriding, Phase analysis, Hardness, Corrosion

I. INTRODUCTION

The austenitic stainless steel is commonly used in chemical plant, food industries and corrosive environment because of its excellent corrosion resistance property. The tribological industrial applications of this steel is limited due to relatively lower wear resistance and hardness. Hence, to make it wide applicable for industrial purpose, the surface properties is generally modified by using techniques like thermal nitriding, carburizing, PVD and CVD coating, plasma source ion implantation, plasma immersion ion implantation and plasma nitridingetc. Among these techniques, plasma nitriding is showing better improvement in mechanical and tribological properties without losing the corrosion resistance properties and damaging the surface finish of the component [1-4].Recent study shows that the stainless steel with improved surface properties could be an alternative choice of graphite for bipolar plate application in fuel cell.

The functions of the bipolar plates in the fuel cell are (i) to separate the reaction gas, (ii) channeling the reactive gas, (iii) providing supports to the membrane electrode assembly,(iv) bringing fuel to anode and oxygen to cathode, and (v) working as a current collector for the electrons available in electrochemical reaction [5, 6]. The functionality can only be achieved if the materials stand with the properties like high electrical conductivity to minimize power loss, good corrosion resistance, high gas impermeability and good mechanical strength [7, 8]. Additionally, it must be inexpensive and low processing cost involvement along with minimal volume and weight because it accounts about eighty percentage of total weight and about forty five percentage of stack cost [9].

Moreover, the graphite and its composites were conventionally used as a bipolar plate material due to low interfacial contact resistance (ICR) and high corrosion resistance. But,high machining cost, low mechanical strength, brittle in nature and large volume of graphite bipolar plates limits the commercialization of the fuel cell

[10]. Therefore, the development of suitable light materials easy to construction and design the bipolar plates possessing ideal characteristic are the key issue for the commercial application. In this regard, stainless steel of 316 grade is regarded as an alternative materials for bipolar plates due to low corrosion resistance in acidic medium, superior manufacturability, cost effectiveness, low gas permeability, higher mechanical strength, better durability to shock and vibration[11].The formation of passive layer and the dissolution of corrosion product in catalyst increase the ICR and decreases the efficiency of the fuel cell [12]. Hence, the further attempt has been taken by various researchers to enhance the corrosion current density and also improve the ICR in order to meet the Department of Energy (DOE) 2020 technical targets of 1 μAcm^{-2} (0.5 M H_2SO_4 + 5 ppm HF, 70°C) and 10 $m\Omega cm^2$ at compaction pressure of 1.5 MPa [13].

Furthermore, it is also reported that the surface modification of steel with metal nitride significantly improves the surface hardness,corrosion current density and ICR. The surface modification perform below 550°C enhanced the surface hardness about three to four fold than base materials [1, 2] and improves the corrosion properties considerably. For example, CrN coated (4.5 mm thick) 316L steel achieved current density (I_{corr}) about 10 $\mu Acm^{-2}$and ICR about 30 $m\Omega cm^2$[14],Cr_2N films (2 mm thick) achieved $I_{corr}$and ICR of 1.77 μAcm^{-2} at 0.6 V (1 M H_2SO_4 + 2 ppm HF, 80°C) and 50 $m\Omega cm^2$at 1.5 MPa respectively[15]. A coating ofCr_xN film on 316L sheets showed I_{corr} about 5 μAcm^{-2} at 0.6 V (0.5 M H_2SO_4 + 5 ppm HF, 70°C) and ICRabout 6.9-10.0 $m\Omega cm^2$under 0.8-1.2 MPa. [16]. Further amorphous carbon coating on CrN coated 316L steel results enhanced $I_{corr}$of 3.56 μAcm^{-2} at 0.6 V and contact resistance of 8.3-5.2 $m\Omega cm^2$ under 1.2-2.1 MPa than CrN coated 316L steel [17].On other hand, TiN has been well established materials for coating the cutting tool because of their high wear resistance, hardness and low friction coefficient characteristics [18]. Subsequently, it is also observed that TiN coating shows very good corrosion resistance and metal-like electrical conductivity [19].

However, little attention has been paid to determining the corrosion performance of TiN coatings on a metallic substrate under fuel cell environmental conditions. There is no report available on the study of corrosion behavior of TiN coated plasma nitride 316 stainless steel. Hence, the present study was aim to develop a hybrid coating on austenitic 316 stainless steel base materials for improving the mechanical and corrosion current density. In this regard, the austenitic 316 stainless steel has been selected as a base materials and which was plasma nitrided at 500°C. Thereafter, the TiN was coated on plasma nitridedaustenitic 316 stainless steel sample using RF magnetron sputtering. The structural, mechanical hardness and corrosion resistance of surface modified 316 stainless steel was investigated in order to improve the protective ability for bipolar plate applications. After surface modification, the phase formation, diffusion layer thickness, surface hardness, and the corrosion properties have been analyzed using X-ray diffraction (XRD), optical microscopeand SEM, nanoindenterand Electrochemical analyzer, respectively.

II. EXPERIMENTAL PROCEDURE

A. Materials and sample preparation

Commercial AISI 316 austenite stainless steel of chemical compositions (C: 0.03, Cr: 16.00-18.00, Ni:10.00-14.00, Si:0.8, Mn:1.7, S:0.030, P:0.045, and Balance Fe) was selected as a base materials for the present investigation. The stainless steel sheets of 1.5 mm thickness were cut into specimens of 10×10 mm size in square shape. The specimen were grounded with SiC papers from #80 up to #1200 grit and polished mechanically with 1 µm diamond paste. The polished specimens were washed with acetoneand dried at room temperature.

B. Plasma nitridingprocess and Titanium nitride film deposition

Glow discharge plasma nitriding process was carried out in anautomated bell shaped stainless steel vacuum chamberusing a D.C. pulsed power supply. The mechanically prepared surface finished samples were placed on the sample holder in the reactor. After that, the vacuum chamber was evacuated to a base pressure of 1 mbar for sputter cleaning. Prior to the plasma nitriding, the samples were sputter cleaned in presence of Arand H_2atmosphere for 1hat 250°C to remove the native oxide layer if present and expose the surface for plasmanitriding. The plasma nitriding was carried out in presence of 80% Nitrogen (N_2) and 20% Hydrogen (H_2) under a pressure of 3 mbar at 500°C for 5 h.After plasma nitriding, the samples were cooled in same atmosphere up to room temperature. Thereafter, the nitrided sample were transferred into RF-magnetron sputtering unit made by Plasma consult, Germany for TiN film deposition. In this process, a typically Ti target of two inch were sputtered in presence ofAr and N_2 (1:1) mixture at at 5 $\times 10^{-2}$ mbar for 2h.

III. CHARACTERIZATION PROCEDURE

A. Structural analysis

The phase analysis ofuntreated, plasma nitrided and TiN coated plasma nitride 316 steel were analyzed by using Powder x-ray diffraction (XRD) with a Bruker D8 Advance x-ray diffractometer.The X-ray diffraction (XRD) studies was carried out using Cu anode X-ray tube, operated at 40 kVand 40 mA to get Cu Kα radiation (λ=1.5406 Å). The diffraction patterns were obtained in the 2θ ranges of 30-90° with the step size of 0.02° and counting time of 1 s per step. The case depth of the nitrided layer was revealed by using a 2% Nital etchant and

examined with a Liecamade optical microscope at a magnification of 100X.The TiN layer was examined using Scanning electron microscope (SEM), Jeol, Japan, Model JSM-6390LV.

B. Nanoindentation Testing

The nanoindentation measurements were performed to measure the surface hardness of untreated, plasma nitrided and TiN coated plasma nitride 316 stainless steel samples by using Nano-indenter, CETR Brucker, model DFH5, USA. Prior to the indentation, the sample was kept under the AFM and an appropriate area was chosen for indentation. Indentations were made on the desired area using a Berkovich diamond indenter of 100 nm tip radius. Multi-cycling progressive load and depth control nanoindentation methods have been used to evaluate the surface hardness properties of the samples.

C. Electrochemical analysis

Corrosion behavior of untreated, plasma nitrided and TiN coated plasma nitrided 316 stainless steel samples were carried out by potentiodynamic test in 0.5M H_2SO_4solution in astimulated environment by conventional three electrode system. The potentiodynamic test were conducted with CH instrument, USA, model 680B electrochemical workstation equipped with CHI660B software controlled by a computer. In this test, the samples was worked as a working electrode, platinum as a counter electrode and Ag/AgCl electrode as the reference electrode. A copper wire was connected to backside of the all samples for electrical connection and further backside of the samples were covered with insulating epoxy. Untreated surface,nitrided surface and TiN coated surface were exposed to solution for electrochemical measurements. Prior to the corrosion tests, all the samples were stabilized at open circuit potential for 30 min, and then the potential was swept from -1.2 V to 1.2 V (vs. SHE), below open circuit potential at a scanning rate of 1 mVs^{-1}. In order to evaluate the stability of the samples, Potentiostatic experiments were conducted for approximately 1000 seconds in the solution as a function of time under PEMFCs operation conditions.

IV. RESULTS AND DISCUSSION

A. Phase analysis

X-ray diffraction patterns of untreated, plasma nitrided and TiN coated AISI 316 austenite stainless steel samples are shown in Fig. 1. The untreated 316 sample (Fig. 1a) displays total three characteristic γ-phase peaks. These observed peaks correspond to the (111), (200), and (220) reflection planes [20]. After plasma nitriding, the CrNpeaks are observed along with small displacement in γ (111) peak towards higher diffraction angle as shown in Figure 1(b).Figure 1(c) shows the diffraction peaks of TiN phase that corresponds to the (111) and (200) planes of TiN, and the intensity of the γ-phases is decreased in comparison to uncoated plasma nitride sample. The decrease in intensity confirms the TiN coating is thin.In Figure 1(c), the diffraction peaks of (111) plane is strongest in present case that of (200) plane in standard diffraction pattern [21]. Further the intensity ratio (111)/(200) is about 1.5 times higher than standard ratio.Thus, the growth orientation of the TiN was mainly in the (111) direction, which is consistent with the findings of other researchers [22-24]. The interplaner spacing (d) of all the observed γ-peaks are calculated using Bragg's equation $2d\ Sin\theta = n\lambda$. With plasma nitriding, the d-value is decreased from 0.20742 nm for untreated to 0.20711 nm for plasma nitrided. The reduction in d-value is probably due to compressive stress resulting from CrN phase segregation on the surface of the steel sample. Using Debye Scherer formula, the TiN crystallite size of 200 nm was estimated.

B. Nitride and TiN layer thickness

Figure 2 shows the surface images of austenitic 316 stainless steel after plasma nitridng and TiN coating, nitride depth and TiN coating thickness. Figure 2 (b) shows the golden color surface image taken from the TiN coated plasma nitrided sample surface. This is the characteristics color of TiN coating. The nitrogen diffusion about 8-10 μm measured from optical microscope is shown in Figure 2(c). Further the SEM image of the TiN and nitride layer is shown in Figure 2(d). The TiN layer thickness about 200 nm and nitride layer about 10 μm is observed.

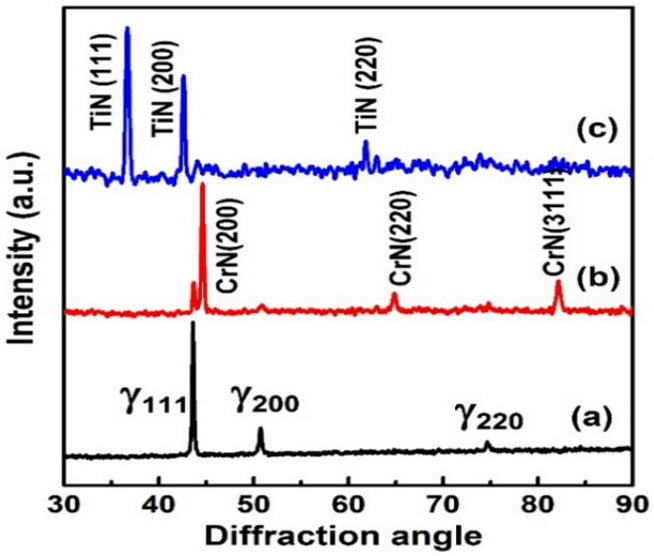

Fig. 1. X-ray diffraction patterns of (a) untreated (b) plasma nitrided and (c) TiN coatedplasma nitrided austenitic 316 stainless steel.

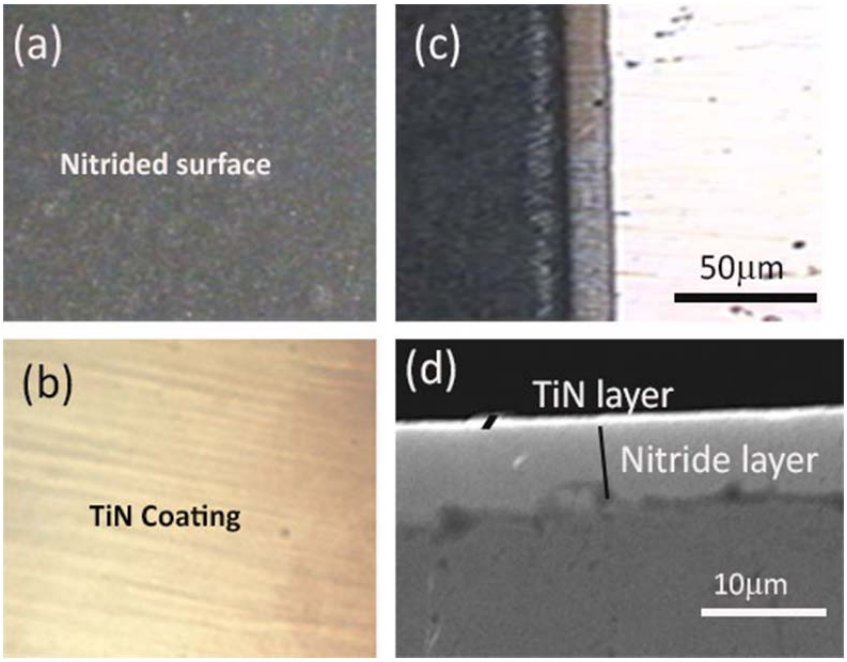

Fig.2.Surfaceimage of austenitic 316 steel after (a)plasma nitridingand (b) TiN coating on plasma nitrided surface; (c) optical image of nitride depth;and (d) SEM image of TiN and nitride layer.

C. Surface hardness

The nanohardness of the untreated, plasma nitrided and TiN coated plasma nitrided austenitic 316 stainless steel was measured using a nanoindenter by applying a uniform load of 2 to 25 mN. The hardness values as a function of penetration depth for these samples are displayed in Figure 3. All samples shows the decreasing trend of hardness with the penetration depth. In Figure 3 (a), the hardness of untreated 316 steel is in the range of 1. 59 to 1.88 GPa. The untreated samples shows initially a maximum hardness of about 1.88 GPa which could be contributed due to stress induced near the surface during sample preparation. After plasma nitriding, the nanohardness values is enhanced and lies in the range of 2.92 to 8.45 GPa which is two to five times higher than untreated sample. The enhancement in hardness in nitrided sample is due to formation of CrN phase at the surface of 316 steel as observed in X-ray pattern in Figure 1(b) [1]. The surface hardness is further enhanced after TiN coating. The value of the surface hardness are ranging from 3.46 to 13.16 GPa as depicted in Fig. 3(c). The enhancement in hardness could be explained on the basis of the stress gradients arising from two competing stress generation mechanism, namely growth-induced point defects known as compressive stress as a consequence of atomic peening, and void formation known as tensile stress as a consequence of surface roughness and shadowing effect.

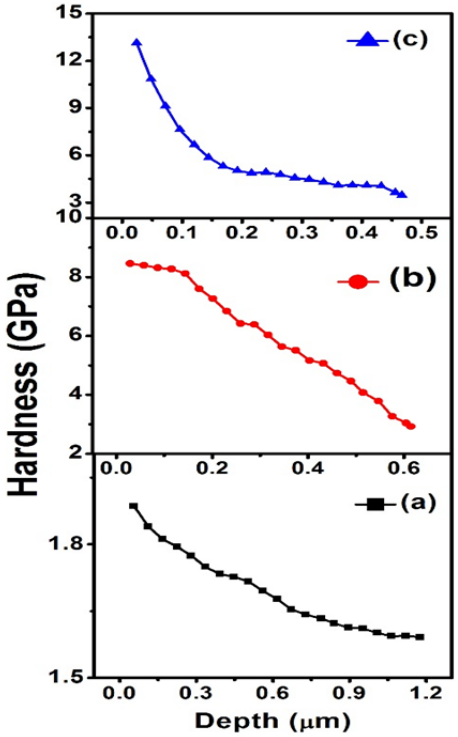

Fig.3. Surface hardness of (a) untreated (b) plasma nitrided and (c) TiN coated plasma nitride austenitic 316 stainless steel

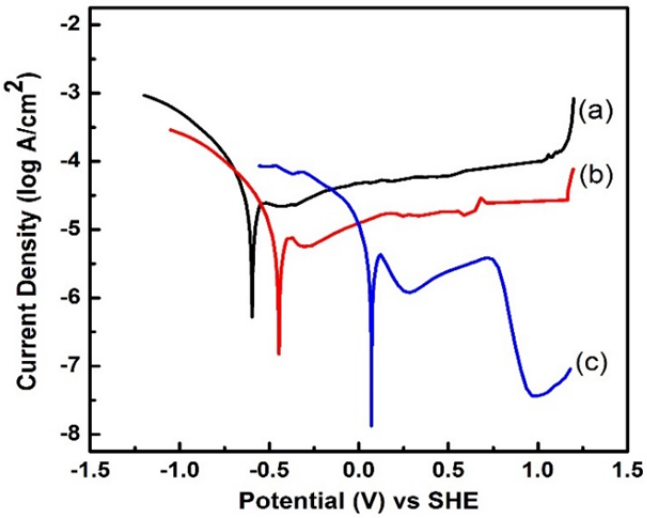

Fig.4.Polarization curve of (a) untreated (b) plasma nitrided and (c) TiN coated Plasma nitrided 316 stainless steel.

D. Electrochemical study

The electrochemical polarization curve of untreated, plasma nitride and TiN coated on plasma nitrided 316 austenite stainless steel samples are portrayed in Figure 4. The polarization curves were recorded in simulated PEMFCs environments through air purging. The activation and passivation turning points in polarization curve supports the formation of passive film on the surface of both plasma nitrided and TiN coated plasma nitrided samples. In Figure 4 (b and c), the corrosion potential (E_{Corr}) of the plasma nitrided and TiN coated plasma nitrided 316 samples showing positive shift with reference to the untreated 316 sample confirms the surface modification impeding the corrosion in the present environment. The obtained E_{Corr} value of untreated, Plasma nitride and TiNcoated plasma nitrided 316 samples are -0.593 V, -0.443 V and 0.074 V, respectively. The corrosion current density (I_{Corr}) is 15.13 μAcm^{-2}, 4.46 μAcm^{-2}, 2.24 μAcm^{-2}, respectively. The passivation current densities of samples measured in the PEMFCs cathodic environment (about 0.6 V vs SHE) are about 69.18 μAcm^{-2}, 18.62 μAcm^{-2} and 3.16 μAcm^{-2}, respectively. The TiN coating significantly improves the current density in comparison to both samples. The enhancement in current density is probably due to smooth TiN coating on the 316 steel surface (as shown in Fig. 2(c) and also the conducting nature of the TiN coating.

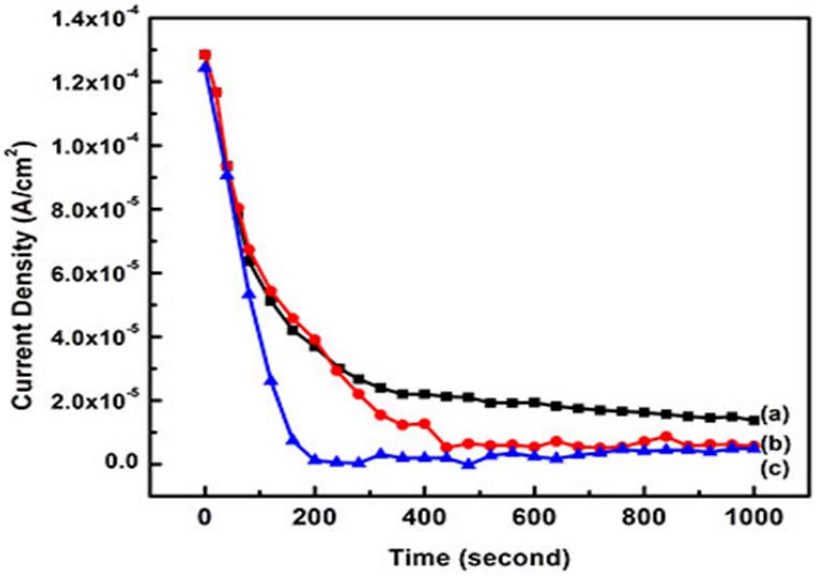

Fig. 5.Potentiostatic curves of (a) untreated (b) plasma nitrided and (c) TiN coated plasma nitridedaustenitic 316 stainless steel

Furthermore, the stability of untreated, plasma nitrided and TiN coated plasma nitrided 316 stainless steel samples were analysed by performing potentiostatic test in simulated environment solution for 1000 seconds. The current density measured as a function of operating time from the potentiostatic polarization test are shown in Fig. 5. In Figure 5, it can be seen that the current density is decreased rapidly when potential was applied. Initially, the current density of all samples decreases in the beginning and gradually stabilizes at a lower current density which implies that the a stable passive film is formed on the surface of the samples. The current density of the untreated sample stabilized in the range of 1×10^{-5}Acm^{-2}, plasma nitride in the range of 4×10^{-6}Acm^{-2} and TiN coated plasma nitride in the range of 8×10^{-7}Acm^{-2}. The stabilization current density of plasma nitrided sample is one order of magnitude lower than that of untreated sample. However, for TiN coated plasma nitrided, it is two order of magnitude lower than that of untreated sample.

V. CONCLUSIONS

The surface modification of the austenitic 316 stainless steel was successfully carried out in two different stages, i.e, using dc glow discharge plasma nitriding at 500°C under 3 mbar pressures for 5 h in the presence of N_2:H_2 gas mixtures of 4:1 ratios and RF magnetron sputtering for titanium nitride (TiN) coating. The bare austenitic 316 stainless steel shows only pure γFe characteristic peaks. After plasma nitriding the new phase CrN is formed. The growth of the TiN particles in <111> direction is identified from X-ray diffraction. The nitrogen diffusion depth of is about 10 μm and the thickness of TiN layer is about 200 nm. Plasma nitriding enhanced the hardness about five times (8.45GPa) whereas the TiN coating about seven times (13.16 GPa) than untreated samples (1.88GPa). The potentiodynamic result shows the positive shift in the corrosion potential (E_{Corr}) after surface treatment. The TiN coating considerably enhanced the corrosion current density (I_{Corr}) to 2.24 μAcm^{-2} from 15.13 μAcm^{-2} for untreated stainless steel. The passivation current densities of after TiN coating measured at 0.6 V vs SHE is 3.16 μAcm^{-2}.

REFERENCES

[1] G. P. Singh, J. Alphonsa, P.K. Barhai, P. A. Rayjada, P. M. Raole, S. Mukherjee, Effect of surface roughness on the properties of the layer formed on AISI 304 stainless steel after plasma nitriding, Surf. Coat. Technol. 200 (2006) 5807-5811.

[2] G. P. Singh, A. Joseph, P. M. Raole, P. K. Barhai, S. Mukherjee, Phase formation in selected surface-roughened plasma-nitrided 304 austenite stainless steel, Sci. Technol. Adv. Mater. 9 (2008) 025007-0250012.

[3] R. Günzel, M. Betzel, I. Alphonsa, B. Ganguly, P. I. John, S. Mukherjee, Plasma-source ion implantation compared with glow-discharge plasma nitriding of stainless steel, Surf. Coat. Technol. 112 (1999) 307-309.

[4] E. Menthe, K.T. Rie, Further Investigation of the structure properties of austenitic stainless steel, after plasma nitridng, Surf. Coat. Technol. 116-119 (1999) 199-204.

[5] I. Nitta, S. Karvonen, O. Himanen, M. Mikkola, Modelling the Effect of Inhomogeneous Compression of GDL on Local Transport Phenomena in a PEM Fuel Cell, Fuel Cells 8 (2008) 410-421.

[6] M. Omrani, M. Habibi, R. Amrollahi, A. Khosravi, Improvement of corrosion and electrical conductivity of 316L stainless steel as bipolar plate by TiN nanoparticle implantation using plasma focus, Int. J. hydrogen energy 37 (2012) 14676-14686.

[7] R. A. Antunes, M. C. L. Oliveira, G. Ett, V. Ett, Corrosion of metal bipolar plates for PEM fuel cells: A review, Int. J. Hydrogen Energy 35 (2010) 3632-47.

[8] Y. Tang, W. Yuan, M. Pan, Z. Wan, Feasibility study of porous copper fiber sintered felt: A novel porous flow field in proton exchange membrane fuel cells, Int. J. Hydrogen Energy 35 (2010) 9661-77.

[9] J. Scherer, D. Münter, R. Ströbel, Influence of Metallic Bipolar Plates on the Durability of Polymer Electrolyte Fuel Cells , in: F. N. Büchi, , M. Inaba, Thomas J. Schmidt (Eds), Polymer electrolyte fuel cell durability, Springer, 2009, p. 243-55

[10] P. Yi, L. Peng, T. Zhou, H. Wu, X. Lai, Cr-N-C multilayer film on 316L stainless steel as bipolar plates for proton exchange membrane fuel cells using closed field unbalanced magnetron sputter ion plating, Int. J. Hydrogen Energy 38 (2013) 1535-1543.
[11] W. Yoon, X. Huang, P. Fazzino, K. L. Reifsnider, M. A. Akkaoui, Evaluation of coated metallic bipolar plates for polymer electrolyte membrane fuel cells, J. Power Sources 179 (2008) 265-73.
[12] M. C. Lopes de Oliveira, G. Ett, R. A. Antunes, Materials selection for bipolar plates for polymer electrolyte membrane fuel cells using the Ashby approach, J. Power Sources 206 (2012) 3-13.
[13] Technical plan-fuel cells, U.S. Department of Energy, 2011.3.4-18.
[14] R. J. Tian, Chromium nitride/Cr coated 316L stainless steel as bipolar plate for proton exchange membrane fuel cell, J. Power Sources 196 (2011) 1258-63.
[15] D. G. Nam and H. C. Lee, Thermal nitridation of chromium electroplated AISI316L stainless steel for polymer electrolyte membrane fuel cell bipolar plate. J. Power Sources 170 (2007) 268-74.
[16] Y. Fu, M. Hou, G. Q. Lin, J. B. Hou, Z. G. Shao, B. L. Yi, Coated 316L stainless steel with CrxN film as bipolar plate for PEMFC prepared by pulsed bias arc ion plating, J. Power Sources 176 (2008) 282-6.
[17] K. Feng, Y. Shen, H. L. Sun, D. A. Liu, Q. Z. An, X. Cai, Conductive amorphous carbon-coated 316L stainless steel as bipolar plates in polymer electrolyte membrane fuel cells, International Journal of Hydrogen Energy 34 (2009) 6771-7.
[18] Y. Li, L. Qu, F. Wang, The electrochemical corrosion behavior of TiN and (Ti, Al) N coatings in acid and salt solution, Corros. Sci. 45 (2003) 1367-1381.
[19] M. Li, S. Luo, C. Zeng, J. Shen, H. Lin, C. Cao, Corrosion behavior of TiN coated type 316 stainless steel in simulated PEMFC environments, Corros. Sci. 46 (2004) 1369-1380.
[20] H.E. Swanson, International Centre for Diffraction Data (ICDD), Nat. Bur. Stand (U.S.), Circ. 4 (1955) 509.
[21] W. Wong, H. McMurdie, B. Paretzkin, C. Hubbard, A. Dragoo, Standard X-Ray Diffraction Powder Patterns of Sixteen Ceramic Phases, Powder Diffraction 2 (1987) 191-202.
[22] C. Hsu, M. Chen, K. Lai, Corrosion resistance of TiN/TiAlN-coated ADI by cathodic arc deposition, Mater. Sci. Eng. A 421 (2006) 182-190.
[23] H.C. Barshilia, M.S. Prakash, A. Poojari, K.S. Rajam, Corrosion behavior of nanolayeredTiN/NbN multilayer coatings prepared by reactive direct current magnetron sputtering process, Thin Solid Films 460 (2004) 133-142.
[24] Y. Wang, D.O. Northwood, An investigation into TiN-coated 316L stainless steel as a bipolar plate material for PEM fuel cells, Journal of Power Sources 165 (2007) 293-298.